

See discussions, stats, and author profiles for this publication at: <https://www.researchgate.net/publication/5313240>

Catalytic Diversity of Extended Hammerhead Ribozymes †

ARTICLE *in* BIOCHEMISTRY · AUGUST 2008

Impact Factor: 3.02 · DOI: 10.1021/bi7025358 · Source: PubMed

CITATIONS

23

READS

16

2 AUTHORS, INCLUDING:



[Irina Shepotinovskaya](#)

Northwestern University

14 PUBLICATIONS 294 CITATIONS

SEE PROFILE

Published in final edited form as:

Biochemistry. 2008 July 8; 47(27): 7034–7042. doi:10.1021/bi7025358.

Catalytic Diversity of Extended Hammerhead Ribozymes†

Irina V. Shepotinovskaya and Olke C. Uhlenbeck*

Department of Biochemistry, Molecular Biology, and Cellular Biology, Northwestern University, 2205 Tech Drive, Hogan 2-100, Evanston, IL 60208

Abstract

Chimeras of the well characterized minimal hammerhead 16 and nine extended hammerheads derived from natural viroids and satellite RNAs were constructed with the goal of assessing whether their very different peripheral tertiary interactions modulate their catalytic properties. For each chimera, three different assays were used to determine the rate of cleavage and the fraction of full length hammerhead at equilibrium and thereby deduce the elemental cleavage (k_2) and ligation (k_{-2}) rate constants. The nine chimeras were all more active than minimal hammerheads and showed a very broad range of catalytic properties, with values of k_2 varying by 750-fold and k_{-2} by 100-fold. At least two of the hammerheads showed an altered dependence of k_{obs} on magnesium concentration. Since much less catalytic diversity is observed among minimal hammerheads that lack the tertiary interactions, a possible role for the different tertiary interaction is to modulate the hammerhead cleavage properties in viroids. For example, differing hammerhead cleavage and ligation rates could affect the steady state concentrations of linear, circular, and polymeric genomes in infected cells.

Keywords

Catalytic RNA; kinetics; RNA tertiary interaction; viroid replication

The hammerhead is a small self-cleaving RNA motif that is found embedded in the genomes of plant viroids and virus satellite RNAs, where it is used for genome cleavage and possibly ligation in a rolling circle replication pathway (1,2). The hammerhead has also been found in the transcripts of certain satellite DNAs (3) and in the 3' untranslated regions of a few *Arabidopsis* mRNAs (4), but its function in these cases remains unknown. Although the conserved catalytic core of the hammerhead was identified in 1987 (5), it was later discovered that all natural hammerheads contain a tertiary interaction between the ends of helices I and II which increases their activity and permits them to function at the low magnesium concentrations present inside cells (6,7). A crystal structure of such an “extended” hammerhead shows that the conformation of the catalytic core is very different than that seen in the structures of “minimal” hammerheads which lack the tertiary interaction (8).

Among the about 30 available sequences of natural hammerheads (3,4,9), the nucleotides in the catalytic core are predominantly conserved with only nucleotides 1.1 (U, C or A), 3 (C or U) and 7 (U, C, A, or G) showing any variation. In addition, a few hammerheads contain an extra nucleotide between core residues 9 and 10.1 (5,10,11) or 11.1 and 12 (12,13). In contrast to the core, the peripheral elements that make up the tertiary interaction in natural hammerheads are remarkably diverse. They can involve interactions between two hairpins, a hairpin and an

†The project described above was supported by R01GM36944-22 from the National Institutes of Health, and 1C06RR018850-01 from the National Center for Research Resources (NCRR), a component of the National Institutes of Health (NIH). Its contents are solely the responsibility of the authors and do not necessarily represent the official views of NCRR or NIH.

*Corresponding Author: Telephone: 847-491-5139, Fax: 847-491-5444. o-uhlenbeck@northwestern.edu

internal loop, or two internal loops that are located at different positions in helices 1 and 2 (6). There is also considerable variation in both size and sequence of the tertiary features. For example, among the 20 different hammerhead sequences currently available which contain an interaction between two hairpins, the size of the loops vary from 3 to 38 nucleotides and no two hammerheads share the identical pair of loop sequences (9). Not only does this great diversity in tertiary interactions help to explain why their presence was missed for so long, but it also implies that numerous sequences can make a productive tertiary interaction. Indeed, an *in vitro* selection experiment identified numerous additional tertiary interactions not found in biology which also enhanced the cleavage rate (14). Analysis of one of these indicated that it promoted cleavage hundreds of times faster than minimal hammerheads (15).

The goal of this paper is to evaluate whether the sequence diversity observed among natural hammerheads results in any difference in their biochemical properties. Although quite different cleavage rates have been reported for several natural hammerheads (7,10,16,17), the reaction protocols differed and the buffer conditions often varied significantly. In addition, in most cases it was not determined whether the extent of cleavage at long incubation reflected the true equilibrium between cleavage and ligation or was reduced by the presence of a fraction of catalytically inactive molecules. If a significant fraction of the hammerheads are misfolded and therefore catalytically inactive, the deduced catalytic rate constants will be incorrectly estimated. This work compares chimeric versions of nine natural hammerheads with differing sequences which all contain hairpins at the ends of helices 1 and 2. Three different assays are used to assess their activities and estimate the fraction of active molecules. We clearly establish that each extended hammerhead has a unique set of catalytic properties.

Materials and Methods

RNA synthesis

The natural hammerhead RNA sequences were selected from the Subviral RNA Database (9). All RNAs were *in vitro* transcribed with T7 RNA polymerase using primer-extended synthetic DNAs as templates (modified from (18)). The transcribed and co-transcriptionally cleaved portion of product was purified on denaturing polyacrylamide gels as described previously (19). The uncleaved hammerheads were transcribed at the presence of inhibitory oligonucleotides and [α - 32 P] ATP at 25° C as described previously (6,7,19,20). During elution of the uncleaved transcript, extensive cleavage was observed even at the presence of 5 mM EDTA. To reduce this high level of self-cleavage, gel elution was performed in 40% formamide and 5 mM EDTA. Purified full length hammerheads were stored at -20° C at the presence of 0.2 mM EDTA to prevent cleavage. The 9mer substrate (P1) for the ligation reaction was prepared using the HH16 ribozyme to cleave a 12mer substrate strand (P1-GUC) from Thermo-Fisher (Dharmacon), Boulder, CO as previously described (19). The resulting P1 contained <10% of uncleaved 12mer which was unreactive in ligation and therefore could be used without purification. Since hydrolysis of P1 to P1 2'(3') phosphate results in a slightly faster moving band on denaturing polyacrylamide gels, the absence of this side reaction was confirmed for all the ligation reactions performed in this study.

Kinetics

Ligation assays were performed under single-turnover condition with saturating (1 μ M) ribozyme and a trace concentration (< 10 nM) of [5'- 32 P] P1 as described previously (19,21). Native gels (15% PAG/ 50mM Tris Acetate (pH 7.5), 10mM Magnesium Acetate; loading buffer: 50% sucrose, 0.02% bromophenol blue, and 0.02% xylene cyanol) were used to confirm that all the P1 formed a complex with Rz. $k_{obs}(L)$ measurements of the very fast nHH3 and nHH8 were performed on a quench flow device (Kintek RQF-3). 1 μ M Rz was annealed to trace (<10 nM) [5'- 32 P] P1 in either MES pH 6.0, 0.4 mM EDTA, or 50 mM HEPES, pH 7.3,

0.4 mM EDTA and was loaded into one sample loop. Either 2 mM or 20 mM MgCl_2 in each buffer were loaded into the second sample loop. Reactions were initiated by delivering equal volumes (~15 μL) of both samples into the reaction loop. Reactions were then quenched at the appropriate time by 86 μL of 7 M urea, 50 mM EDTA. From each time point, 16 μL were analyzed by gel electrophoresis. Intramolecular hammerhead cleavage was performed as described previously (6,7,19,20). To determine $k_{\text{obs}}(\text{C})$, full length transcripts were incubated in 50 μL of 50 mM MES, pH 6.0, 0.2 mM EDTA at 95° C for 2 min, slow cooled to 25° C and 50 μL of 2.2 mM MgCl_2 in 50 mM MES (pH 6.0) were added to start the reactions. Reactions were terminated with 3X stop buffer (1X TBE/7 M Urea, 50 mM EDTA, 0.02% of bromophenol blue and xylene cyanol) at different time points and analyzed on 20% PAGE under denaturing conditions. Any RNA that cleaved during purification and preincubation was assumed to cleave during the reaction.

Coupled-transcription-cleavage

The assay was modified from (22) and described in detail in (19). A 25 μL transcription mixture contained 2.5 μg of T7 polymerase, 4 mM of each NTP, 10 μCi of [α - ^{32}P]ATP, 17 mM MgCl_2 and 40 mM Tris-HCl buffer, pH 8.1. Since NTP's and the pyrophosphate product both chelate ions tightly, the final free magnesium concentration remained constant at 1 mM. Reactions were initiated by the addition of 2 μL of 1 $\mu\text{g}/\mu\text{L}$ DNA template. After two hours of incubation at 25° C, 5 μL aliquots were quenched with 3X stop buffer and analyzed on 10% polyacrylamide gels.

Results

The RNA secondary structures and genome abbreviations of the nine natural hammerheads chosen for this work are shown in Figure 1. Seven of these natural hammerheads came from either the plus or minus strands of different viroid or satellite viral genomes while two come from the plus and minus strand of the LTSV genome. The hammerheads were primarily chosen on the basis of having diverse loop 1 and loop 2 sequences; however, extremely large loops were avoided to minimize potential misfolding in the *in vitro* assays. While the cleavage properties of several (including CChMVd, rCSCVd, PLMVd, satTRsV) have previously been investigated biochemically (10,19,23,24), others (including satSCMoV) have only been shown to cleave *in vitro* (25), while still others (including satCYMoV, satArMV) are only proposed to self-cleave based upon their sequence (11,26).

The cleavage and ligation reactions of the nine hammerheads were studied using an approach developed previously for the satTRsV hammerhead (19). As shown for one example in Figure 2, the native helix III of each natural hammerhead was replaced with helix III of HH16, a well-characterized minimal hammerhead, to create a chimera. These chimeras were named nHH1 to nHH9 (Figure 1) where nHH9 is identical to HH16-T2 derived from satTRsV which we studied previously (19). Since the X-ray structure of the extended hammerhead (8) shows that helix III does not interact with any other parts of the hammerhead, this substitution is not expected to influence the catalytic properties of the remainder of the molecule. The primary advantage of using chimeras is that the new helix III is sufficiently stable to permit measurement of the reverse, ligation reaction while the corresponding helices of several of the natural hammerheads (satLTSV, satArMV, and satTRsV) are too weak to allow stable product binding. An additional experimental convenience is that the same labeled product oligonucleotide, P1, can be used to assay all nine hammerheads. Although helix substitutions can cause long range effects on the cleavage rates of ribozymes (27), there is no indication that this occurs for the hammerhead. Numerous substitutions that modify the sequence and length of helix III of minimal hammerheads have not revealed effects on k_{cat} (28,29). Since it is now clear that the minimal hammerhead goes through the same transition state as extended

hammerheads (30,31), it is likely that the cleavage properties of the chimeras will reflect those of the parent molecule.

The catalytic properties of the eight new chimeric hammerheads were initially assayed by measuring the rate and extent of the ligation. This was done by annealing a low concentration of [5'-³²P] labeled P1 to a saturating concentration of Rz, the remainder of each hammerhead (Figure 3A). As was done with HH16 (21), native gels were used to confirm that >95% of the P1 formed a complex with Rz. Ligation of the Rz*P1 complex was then initiated by the addition of the desired concentration of MgCl₂ and the reaction progress followed until equilibrium was reached (Figure 3B). The reaction conditions of 1 mM MgCl₂, 50 mM MES pH 6.0 at 25° C were chosen to give reaction rates that in most cases were slow enough that manual pipetting could be used. FRET and EPR experiments have shown that above 0.5 mM MgCl₂ the *S. mansoni* extended hammerhead adopts the helical orientation seen in the crystal structure (32, 33). In seven of the nine cases, the data fit well to a single observed rate constant, $k_{\text{obs}}(\text{L})$, and a fraction full length molecule at equilibrium, $f_{\text{eq}}(\text{L})$. For nHH3 and nHH8, $k_{\text{obs}}(\text{L})$ was too fast to measure manually, but values of $f_{\text{eq}}(\text{L})$ could be obtained. The results are summarized in Table 1. The values of $k_{\text{obs}}(\text{L})$ varied from 0.024 min⁻¹ to >2.5 min⁻¹ and the $f_{\text{eq}}(\text{L})$ varied from 0.01 to 0.32. While all nine natural hammerheads ligated faster and to a greater extent than the minimal HH16 under the same conditions ($k_{\text{obs}} = 0.004 \text{ min}^{-1}$, $f_{\text{eq}} = 0.0075$), it is clear that this structurally diverse set of extended chimeric hammerheads have diverse catalytic properties.

In order to measure $k_{\text{obs}}(\text{L})$ for nHH3 and nHH8, a rapid quench flow device was used to add MgCl₂ to initiate the reaction and EDTA to terminate the reaction at each desired time point. As summarized in Table 2, nHH3 ligated at 17.3 min⁻¹ and nHH8 at 6.8 min⁻¹ in the buffer used in Table 1. As has been reported for other extended hammerheads (15,16,34), the reaction rate increases with both magnesium ion concentration and pH. At conditions commonly used for minimal hammerheads (10 mM MgCl, pH 7.3), nHH3 shows a $k_{\text{obs}}(\text{L}) = 860 \text{ min}^{-1}$, more than 10³ times faster than the minimal HH16.

The rates and extents of intramolecular cleavage of the chimeric hammerheads were measured in a second set of assays. Intact, uncleaved hammerheads were prepared by performing *in vitro* transcription of a complete hammerhead template in the presence of a complementary DNA oligomer to inhibit co transcriptional cleavage (6,7,19,20). The resulting ³²P-labeled uncleaved full length hammerhead was purified from the inhibitory oligomer on a denaturing gel and then eluted and stored in the absence of divalent ions. After refolding in the reaction buffer, cleavage is initiated by the addition of the desired concentration of MgCl₂. As shown for nHH1 in Figure 3B, the time course of the cleavage reaction can be fit to a single observed rate constant $k_{\text{obs}}(\text{C})$, and a fraction of full length at equilibrium, $f_{\text{eq}}(\text{C})$. However, analysis of these cleavage experiments was often complicated by the presence of a fraction of cleaved molecules in the starting material that presumably arose from cleavage that occurred during the purification and/or the refolding step. This problem was especially acute for hammerheads that cleaved rapidly such as nHH3 and nHH8, so rapid quench experiments were not attempted. The cleavage data for the nine hammerheads are summarized in Table 1. Again the extended hammerheads are all faster than the minimal HH16 and show substantial differences in their cleavage rates and extents.

The ligation and cleavage assays presumably measure the approach to the same equilibrium between cleaved and uncleaved hammerhead from opposite directions. Thus, the value of $k_{\text{obs}}(\text{L})$ should equal $k_{\text{obs}}(\text{C})$ since both reflect the sum of the same forward (k_2), and reverse (k_{-2}) elemental rate constants (29). Furthermore, if both the cleaved and uncleaved hammerheads are fully active, the two assays should also give the same value of f_{eq} . As shown in Table 1, with the exception of the very fast nHH3 and nHH8 where $k_{\text{obs}}(\text{C})$ data are not

available, the values of $k_{\text{obs}}(\text{C})$ and $k_{\text{obs}}(\text{L})$ for each hammerhead indeed agree within a factor of two, indicating that the two assays are measuring the same reaction. However, $f_{\text{eq}}(\text{L})$ and $f_{\text{eq}}(\text{C})$ only match well in three of the nine cases tested (nHH1, nHH6 and nHH8). As discussed previously (19), this poor agreement of f_{eq} values suggests that a fraction of the hammerhead molecules present in the reaction are inactive in one or both assays. In the case of the cleavage assay, incorporation errors in transcription and incorrect folding during purification can result in a fraction of inactive full length molecules. This will result in an observed value of $f_{\text{eq}}(\text{C})$ that is inappropriately high. In the case of the ligation assay, the starting preparation of Rz must have been active since it was obtained from a self-cleavage reaction. However, a fraction of Rz molecules may not have been folded properly after purification from the denaturing gel, resulting in an abnormally low value of $f_{\text{eq}}(\text{L})$. Although different reannealing protocols were tested, the observed disparity between $f_{\text{eq}}(\text{C})$ and $f_{\text{eq}}(\text{L})$ remained a persistent problem for six of the nine hammerheads.

Since it is important to have a reliable value of f_{eq} to dissect the elemental rate constants, a coupled transcription-cleavage assay was used as an alternative way to obtain f_{eq} . In this assay, each chimeric hammerhead was transcribed from a duplex DNA template using T7 RNA polymerase. The reactions were performed at the 1 mM free MgCl_2 concentration used in the other two assays but at a higher pH to permit transcription (19). Since the hammerheads fold and cleave during transcription, they are not subjected to the denaturing conditions used for their purification in the other two assays. This minimizes, but may not eliminate, the potential for a fraction of the molecules misfolding into an inactive conformation. While this assay can be used to obtain cleavage rates (22), the cleavage rates of the extended hammerheads are too fast compared to the rate of transcription, so only the fraction of full length molecules at equilibrium, $f_{\text{eq}}(\text{T})$, was obtained. As shown in Figure 3B for nHH1, the value of $f_{\text{eq}}(\text{T})$ closely matched those of both $f_{\text{eq}}(\text{L})$ and $f_{\text{eq}}(\text{C})$. This agreement between all three assays strongly suggests that both the cleaved and uncleaved forms of nHH1 are fully active. A similar conclusion can be made for nHH6 and nHH8. In the case of nHH2, nHH4 and nHH9, the $f_{\text{eq}}(\text{L})$ and $f_{\text{eq}}(\text{T})$ values agree, suggesting that the disparate $f_{\text{eq}}(\text{C})$ value is the result of a fraction of inactive full length molecules present in the cleavage assay. Finally, for three of the hammerheads (nHH3, nHH5, and nHH7) all three f_{eq} values differ and $f_{\text{eq}}(\text{T})$ lies between $f_{\text{eq}}(\text{L})$ and $f_{\text{eq}}(\text{C})$. In these cases, we assume that inactive molecules are present in both the uncleaved and cleaved hammerhead populations and the correct value of f_{eq} is the one obtained in the transcription assay $f_{\text{eq}}(\text{T})$. However, since we cannot exclude the possibility that misfolding also occurs during transcription, the actual value of f_{eq} for these three poorly folding hammerheads must be considered less certain.

The availability of values for k_{obs} and f_{eq} make it possible to calculate k_2 and k_{-2} , the rate constants for cleavage and ligation since $k_{\text{obs}} = k_2 + k_{-2}$ and $f_{\text{eq}} = k_{-2}/(k_2 + k_{-2})$. As summarized in Table 3, average values of k_{obs} and the best estimate for f_{eq} were used to calculate values for k_2 and k_{-2} for each of the nine hammerheads in 1 mM MgCl_2 , 50 mM MES pH 6.0. All nine chimeric hammerheads show k_2 values that are 5 to 3750-fold faster than the minimal HH16 in the same buffer. Similarly, all the extended hammerheads show values of k_{-2} that are greater than HH16, but also vary considerably (475-fold). Interestingly, although the values of k_2 and k_{-2} correlate with one another, the correlation is not perfect. For example, nHH4 and nHH9 have nearly identical values of k_2 , nHH4 has a nearly five-fold faster k_{-2} . This lack of perfect correlation between k_2 and k_{-2} is also evident in the 13-fold range in the ratio between cleaved and ligated forms at equilibrium that is described by the “internal” equilibrium constants ($K_{\text{int}} = k_2/k_{-2}$) in Table 3.

The ligation assay was used to determine k_{obs} as a function of MgCl_2 concentration for one of the slowest in the selected hammerheads, nHH1, and two of the faster ones, nHH3 and nHH5. Plots for $\log[k_{\text{obs}}]$ versus $\log[\text{MgCl}_2]$ are presented in Figure 4, along with data reported

previously for nHH9 (19) and the minimal HH16 (35). The slopes of the plots for nHH1 and nHH9 are somewhat less than one, similar to the *S. mansoni* hammerhead (16), HH16 (35), an *in vitro* selected extended hammerhead (15) and numerous other minimal hammerheads (36, 37). However, nHH3 and nHH5 show a nearly second order dependence of k_{obs} on MgCl_2 concentration which has only rarely been observed for hammerheads (15). Although many divalent ions bind to the hammerhead the cleavage rate only reports on the binding of the weakest ion needed to reach the transition state. Although it appears that nHH3 and nHH5 utilize two divalent ions of similar affinities to reach the transition state instead of the usual one. It is unclear whether this reflects an additional divalent ion or whether one of the tighter binding divalent ions binds less well to these hammerheads and thereby also becomes rate limiting to reach the transition state.

The ligation assay was also used to determine k_{obs} for the extended hammerheads in 2 M LiCl, pH 7.5 HEPES buffer in the absence of divalent ions. As summarized in Table 4, all of the extended hammerheads are not very active in this buffer, showing k_{obs} values only slightly (2 to 7-fold) faster than reported for the minimal HH16 under the same conditions. Thus, as was previously concluded for nHH9 (19) and the *S. mansoni* hammerhead (16), it appears that the effect of tertiary interaction is much less in LiCl than in buffers containing divalent ions. Either the tertiary interactions do not form in LiCl or a bound magnesium ion is required for rapid hammerhead cleavage.

Discussion

The catalytic properties of nine hammerheads containing different peripheral tertiary interactions were compared under uniform reaction conditions. The hammerheads were chosen from more than 20 natural viroid sequences to have tertiary interactions with relatively small hairpin loops in order to maximize the likelihood that the molecules would fold properly and therefore be active. Although all nine hammerheads showed enhanced cleavage and ligation rates compared to hammerheads lacking the tertiary interaction, in six of the cases the reaction reached a different end point when the equilibrium was approached from opposite directions. This is a clear indication that a significant fraction of the purified full length hammerhead and/or the cleaved product molecules were not active, either because of errors in transcription or because they had misfolded or were inactivated during their purification from denaturing gels. The inability to fully renature RNA molecules is well documented (38) and has previously been observed with both extended (17,39) and minimal (40,41) hammerheads. Thus, out of the nine extended hammerheads tested, only nHH1, nHH6, and nHH8 can be purified in both their cleaved and uncleaved forms as fully active species. These hammerheads are therefore favored candidates for future biochemical and biophysical studies. However three others (nHH2, nHH4 and nHH9), appear to form fully active cleaved forms and therefore can be studied in ligation reactions.

An estimate of the fraction of full length molecules at equilibrium permitted the values for the apparent cleavage (k_2) and ligation (k_{-2}) rate constants to be calculated. It is striking that the values of these rate constants are very fast for some of the chimeras. nHH3, the fastest of the nine tested, has a $k_2 = 15 \text{ min}^{-1}$ in the 1 mM MgCl_2 , pH 6 buffer used in this study, but increases to $>750 \text{ min}^{-1}$ in the 10 mM, pH 7.3 buffer more commonly used for measuring hammerhead cleavage rates. Even faster k_2 values would be expected if the pH, MgCl_2 concentration, or temperature were increased. k_{obs} values in excess of 800 min^{-1} have also been reported for derivatives of the *S. mansoni* hammerhead (16) and the PLMVd hammerhead (15) in slightly different buffers. Since k_2 values of about 1 min^{-1} are typically observed for minimal hammerheads at 10 mM MgCl_2 , pH 7.5 (21,29,41), this emphasizes the importance of the tertiary interaction for stimulating catalysis. In addition, it is now clear that the “speed limit” for RNA catalysis by the hammerhead mechanism is at least 1000-fold faster than previously

thought and even faster cleavage rates may be possible. This may mean that the mechanism is more complex than previously thought (42).

A second striking feature of the data is that the cleavage and ligation rate constants among the group of nine hammerheads tested are quite diverse. Values of k_2 vary from 0.02 min^{-1} to 15 min^{-1} and k_{-2} varies from 0.004 min^{-1} to 1.9 min^{-1} . Since the values of k_2 and k_{-2} roughly correlate, this suggests that a lot of the catalytic diversity is the result of each hammerhead having a slightly different transition state energy. However, since the values of $K_{\text{int}} = k_2/k_{-2}$ vary from 2.4 to 32, this indicates that the relative position of the cleaved and uncleaved ground states in the reaction free energy diagram are also slightly different. In other words, it appears that the differing hammerhead sequences subtly modify the entire hammerhead reaction profile, leading to their diverse catalytic properties.

Which sequence elements in the extended hammerhead are responsible for the differing catalytic properties? While the catalytic cores of nHH1 to nHH9 are not identical, the observed sequence variations at position 7 (U, G, or A) are not expected to significantly modify rates based on experiments with minimal hammerheads (43). A residue that is likely to be responsible for some of the catalytic diversity is the “bulged” nucleotide positioned between A9 and G10 (9), which substantially enhances cleavage of minimal hammerheads (10,44) and is present in the three fastest hammerheads studied here (nHH3, nHH5 and nHH8). Another source of catalytic diversity could be the varying sequence at the base pairs 1.1-1.2 and 2.1-2.2 which can modify cleavage rates in minimal hammerheads about 10-fold (45). Finally, since it is clear that the tertiary interaction dramatically stimulates the catalytic activity, it also may contribute to the diversity in activities. The X-ray structure suggests that the tertiary interaction helps to stabilize the catalytically active core conformation by underwinding helix II and overwinding helix I (8). Thus, the structural details of the tertiary interaction as well as the length and sequence of the two helices could potentially affect the structure and/or dynamics of the core and therefore how easily the transition state can be reached. Since the structure and dynamics of the cleaved and uncleaved forms of the hammerhead are likely to be different, each tertiary interaction may affect ground state energies of these forms somewhat differently, leading to different K_{int} values.

An alternate source of catalytic diversity among the different extended hammerheads may be in their differential ability to form the functional tertiary interaction. As originally proposed by Perrachi and Herschlag (46,47), it is now clear that although minimal hammerheads normally adopt a catalytically inactive conformation, they transiently form the same core structure as the extended hammerhead before and after cleavage. Since these conformational isomerizations are very fast compared to the cleavage rate, k_{obs} and f_{eq} can be described by:

$$k_{\text{abs}} = \left(\frac{K_u}{1+K_u} \right) k'_2 + \left(\frac{1}{1+K_c} \right) k'_{-2}$$

$$f_{\text{eq}} = \left(\frac{1}{1+K_c} \right) \frac{k'_{-2}}{k_{\text{obs}}}$$

where K_u and K_c are the equilibrium constants describing the conformational change between the inactive and active conformations of the uncleaved and cleaved hammerhead and k'_2 and k'_{-2} reflect the “true” elemental rate constants of cleavage and ligation and may be the same for all hammerheads (30). While K_u and K_c are likely to strongly favor the inactive conformations for minimal hammerheads, and strongly favor the active conformation for the

very fast extended hammerheads, it is possible that the slower extended hammerheads have intermediate values of K_u and K_c . If this were true, part of the variability of k_{obs} and f_{eq} would be due to the differential ability to form the tertiary interaction. In other words, the slower extended hammerheads may simply have weaker tertiary interactions so that they spend a larger proportion of their time in a conformation that may resemble the catalytically inactive minimal hammerhead structure.

No matter what the underlying structural basis of the catalytic diversity among natural hammerheads turns out to be, it is important to consider why each viroid species has acquired a hammerhead with different sequence and catalytic properties. As with viruses, the small genomes of viroids and satellite RNA are probably highly evolved to fit their individual complex biological niches. Indeed, viroid mutations are often less infectious than their wild type counterparts and are rapidly lost upon propagation (48-50). It therefore seems unlikely that the hammerhead present in a given viroid was simply “frozen” in evolution as one of the many equivalent alternatives, but rather that it was selected to optimize the fitness of the viroid. Hammerheads play a critical role in the replication of viroid genomes by cleaving positive and negative strand genome multimers generated in their replication pathway (1). The resulting linear genome monomers are cyclized in a ligation reaction that in some cases may also be catalyzed by the hammerhead (51) and in others by a cellular RNA ligase (52). The resulting circles are used as templates for generating multimers by a rolling circle mechanism (53,54). Analysis of the reaction intermediates by northern blots indicate that the relative amounts of positive and negative strand multimer, monomer and circular genomes differ dramatically among different viroids. For example, sASBV infected cells accumulate primarily positive strand genome multimers and monomer circles (55) while PLMVd accumulates roughly equal amounts of positive and negative strand linear monomers and relatively few genome multimers or circles (54).

It is possible that the differing catalytic properties of hammerheads present in different viroids could influence the relative steady state concentrations of the reaction intermediates. For example, hammerheads with fast k_{obs} and a low f_{eq} values could accumulate linear monomer intermediates, while viroids with hammerheads with slower k_{obs} and greater f_{eq} values could accumulate more multimers or circles. However, there are several reasons why it is inappropriate to directly correlate the data presented here with the northern blot data. First, since we have measured rates using chimeric hammerheads under nonphysiological conditions, the cleavage and ligation rates of the natural hammerhead sequences *in vivo* may be considerably different. Second, hammerhead sequences embedded in viral genomes may only transiently fold into an active conformation and then rearrange to an entirely different structure, thereby giving a substantially different f_{eq} than determined with an isolated hammerhead. Finally, the different forms of viroid genomes could be degraded at different rates, so their relative steady state concentrations may not relate to hammerhead cleavage rates in any simple way. Nevertheless, our observation that different natural hammerheads can have very different intrinsic abilities to cleave and ligate suggests an additional mechanism for how the viroid genome could control its replication pathway.

Abbreviations

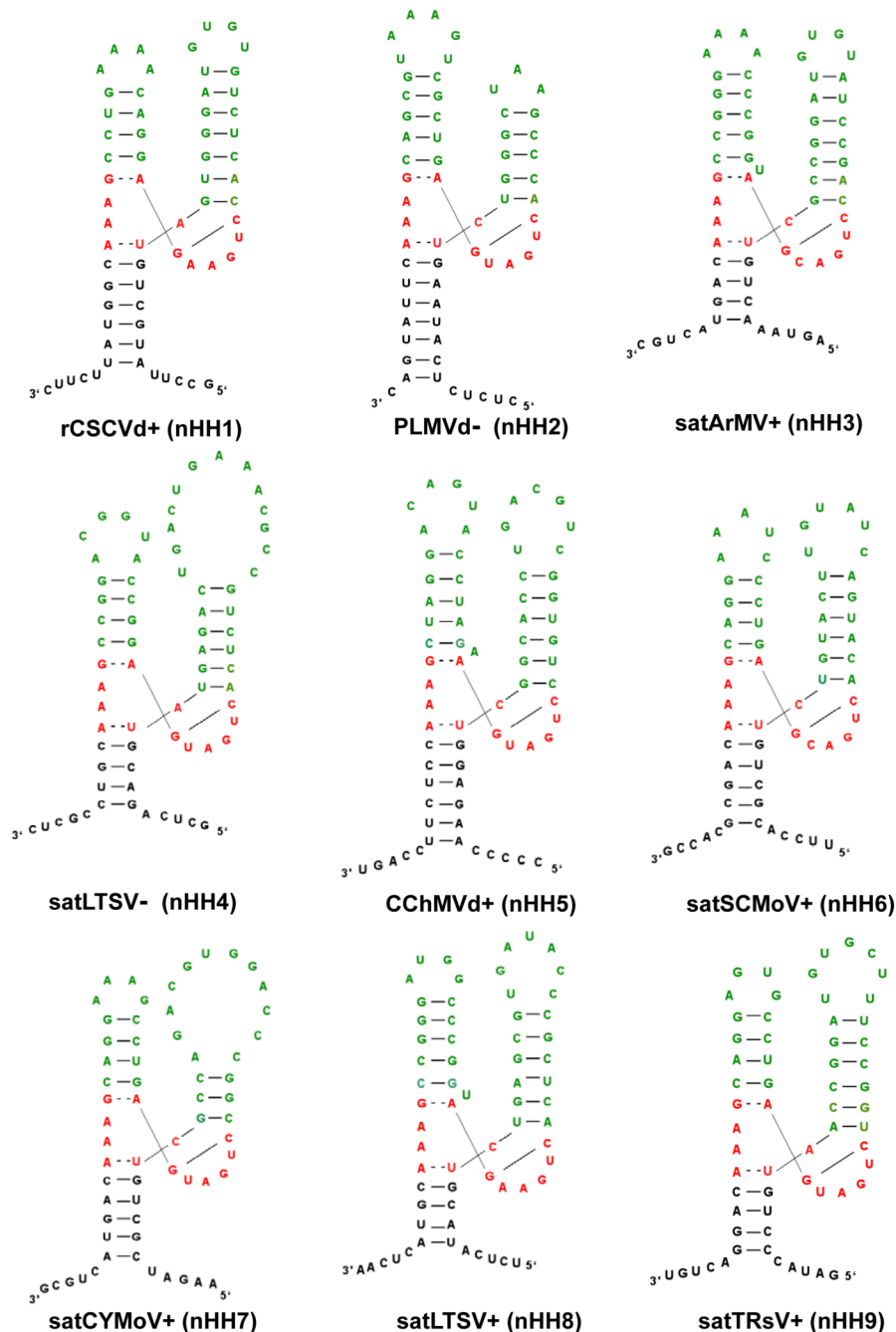
HH, Hammerhead ribozyme; EPR, electron paramagnetic resonance; Rz, ribozyme; HEPES, *N*-(2-hydroxyethyl)piperazine-*N'*-2-ethanesulfonic acid; PAGE, polyacrylamide gel electrophoresis; MES, 2-(*N*-morpholino)ethanesulfonic acid; FRET, fluorescence resonance energy transfer; NTP, Nucleotide Triphosphate; EDTA, ethylenediaminetetraacetic acid.

References

1. Symons RH. Plant pathogenic RNAs and RNA catalysis. *Nucleic Acids Res* 1997;25(14):2683–2689. [PubMed: 9207012]
2. Flores R, Di Serio F, Hernandez C. Viroids: the non coding genomes. *Semin. Virol* 1997;8:65–73.
3. Epstein LM, Gall JG. Self-cleaving transcripts of satellite DNA from the newt. *Cell* 1987;48:535–543. [PubMed: 2433049]
4. Przybilski R, Graf S, Lescoute A, Nellen W, Westhof E, Steger G, Hammann C. Functional hammerhead ribozymes naturally encoded in the genome of *Arabidopsis thaliana*. *Plant Cell* 2005;17:1877–1885. [PubMed: 15937227]
5. Forster AC, Symons RH. Self-cleavage of plus and minus RNAs of a virusoid and a structural model for the active sites. *Cell* 1987;49(2):211–220. [PubMed: 2436805]
6. Khvorova A, Lescoute A, Westhof E, Jayasena SD. Sequence elements outside the hammerhead ribozyme catalytic core enable intracellular activity. *Nat. Struct. Biol* 2003;10(9):708–712. [PubMed: 12881719]
7. De la Pena M, Gago S, Flores R. Peripheral regions of natural hammerhead ribozymes greatly increase their self-cleavage activity. *EMBO J* 2003;22(20):5561–5570. [PubMed: 14532128]
8. Martick M, Scott WG. Tertiary contacts distant from the active site prime a ribozyme for catalysis. *Cell* 2006;126:309–320. [PubMed: 16859740]
9. Rocheleau L, Pelchat M. The Subviral RNA Database: a toolbox for viroids, the hepatitis delta virus and satellite RNAs research. *BMC Microbiol* 2006;6:24. [PubMed: 16519798]
10. De la Pena M, Flores R. An extra nucleotide in the consensus catalytic core of a viroid hammerhead ribozyme: implications for the design of more efficient ribozymes. *J Biol Chem* 2001;276:34586–34593. [PubMed: 11454858]
11. Kaper JM, Tousignant ME, Steger G. Nucleotide sequence predicts circularity and self-cleavage of 300-ribonucleotide satellite of arabis mosaic virus. *Biochem Biophys Res Commun* 1988;154:318–325. [PubMed: 3395334]
12. Hernandez C, Daros JA, Elena SF, Moya A, Flores R. The strands of both polarities of a small circular RNA from carnation self-cleave in vitro through alternative double- and single-hammerhead structures. *Nucleic Acids Res* 1992;20:6323–6329. [PubMed: 1282239]
13. Song SI, Silver SL, Aulik MA, Rasochova L, Mohan BR, Miller WA. Satellite cereal yellow dwarf virus-RPV (satRPV) RNA requires a double hammerhead for self-cleavage and an alternative structure for replication. *Journal of molecular biology* 1999;293:781–793. [PubMed: 10543967]
14. Saksmerprome V, Roychowdhury-Saha M, Jayasena S, Khvorova A, Burke DH. Artificial tertiary motifs stabilize trans-cleaving hammerhead ribozymes under conditions of submillimolar divalent ions and high temperatures. *Rna* 2004;10:1916–1924. [PubMed: 15547137]
15. Roychowdhury-Saha M, Burke DH. Extraordinary rates of transition metal ion-mediated ribozyme catalysis. *Rna* 2006;12:1846–1852. [PubMed: 16912216]
16. Canny MD, Jucker FM, Kellogg E, Khvorova A, Jayasena SD, Pardi A. Fast cleavage kinetics of a natural hammerhead ribozyme. *J. Am. Chem. Soc* 2004;126(35):10848–10849. [PubMed: 15339162]
17. Przybilski R, Hammann C. Idiosyncratic cleavage and ligation activity of individual hammerhead ribozymes and core sequence variants thereof. *J. Biol. Chem* 2007;388:737–741.
18. O'Rear JL, Wang S, Feig AL, Beigelman L, Uhlenbeck OC, Herschlag D. Comparison of the hammerhead cleavage reactions stimulated by monovalent and divalent cations. *Rna* 2001;7:537–545. [PubMed: 11345432]
19. Nelson JA, Shepotinovskaya I, Uhlenbeck OC. Hammerheads derived from sTRSV show enhanced cleavage and ligation rate constants. *Biochemistry* 2005;44:14577–14585. [PubMed: 16262257]
20. Carbonell A, De la Pena M, Flores R, Gago S. Effects of the trinucleotide preceding the self-cleavage site on eggplant latent viroid hammerheads: differences in co- and post-transcriptional self-cleavage may explain the lack of trinucleotide AUC in most natural hammerheads. *Nucleic Acids Res* 2006;34:5613–5622. [PubMed: 17028097]
21. Hertel KJ, Herschlag D, Uhlenbeck OC. A kinetic and thermodynamic framework for the hammerhead ribozyme reaction. *Biochemistry* 1994;33:3374–3385. [PubMed: 8136375]

22. Long DM, Uhlenbeck OC, Department of, C.; Biochemistry, U. o. C. B. Kinetic characterization of intramolecular and intermolecular hammerhead RNAs with stem II deletions. *Proc. Nat. Acad. Sci. USA* 1994;91(15):6977–6981. [PubMed: 7518924]
23. Hernandez C, Flores R. Plus and minus RNAs of peach latent mosaic viroid self-cleave in vitro via hammerhead structures. *Proc Natl Acad Sci U S A* 1992;89:3711–3715. [PubMed: 1373888]
24. Di Serio F, Daros JA, Ragozzino A, Flores R. A 451-nucleotide circular RNA from cherry with hammerhead ribozymes in its strands of both polarities. *J Virol* 1997;71:6603–6610. [PubMed: 9261382]
25. Davies C, Haseloff J, Symons RH. Structure, self-cleavage, and replication of two viroid-like satellite RNAs (virusoids) of subterranean clover mottle virus. *Virology* 1990;177:216–224. [PubMed: 1693803]
26. Rubino L, Tousignant ME, Steger G, Kaper JM. Nucleotide sequence and structural analysis of two satellite RNAs associated with chicory yellow mottle virus. *J Gen Virol* 1990;71(Pt 9):1897–1903. [PubMed: 1698918]
27. Tinsley RA, Walter NG. Long-range impact of peripheral joining elements on structure and function of the hepatitis delta virus ribozyme. *Biological chemistry* 2007;388:705–715. [PubMed: 17570823]
28. Fedor MJ, Uhlenbeck OC. Substrate sequence effects on “hammerhead” RNA catalytic efficiency. *Proc Natl Acad Sci U S A* 1990;87:1668–1672. [PubMed: 1689847]
29. Stage-Zimmermann TK, Uhlenbeck OC, Department of, C. Hammerhead ribozyme kinetics. *Rna* 1998;4(8):875–889. [PubMed: 9701280]
30. Nelson JA, Uhlenbeck OC. Minimal and extended hammerheads utilize a similar dynamic reaction mechanism for catalysis. *Rna* 2008;14:43–54. [PubMed: 17998291]
31. Nelson JA, Uhlenbeck OC. Hammerhead Redux: Does the new structure fit the old biochemical data? *Rna*. 2008
32. Penedo JC, Wilson TJ, Jayasena SD, Khvorova A, Lilley DM. Folding of the natural hammerhead ribozyme is enhanced by interaction of auxiliary elements. *Rna* 2004;10:880–888. [PubMed: 15100442]
33. Kim NK, Murali A, DeRose VJ. Separate metal requirements for loop interactions and catalysis in the extended hammerhead ribozyme. *J Am Chem Soc* 2005;127:14134–14135. [PubMed: 16218578]
34. Osborne EM, Schaak JE, Derose VJ. Characterization of a native hammerhead ribozyme derived from schistosomes. *Rna* 2005;11:187–196. [PubMed: 15659358]
35. Clouet-d’Orval B, Stage TK, Uhlenbeck OC. Neomycin inhibition of the hammerhead ribozyme involves ionic interactions. *Biochemistry* 1995;34(35):11186–11190. [PubMed: 7669776]
36. Inoue A, Takagi Y, Taira K. Importance in catalysis of a magnesium ion with very low affinity for a hammerhead ribozyme. *Nucleic Acids Res* 2004;32:4217–4223. [PubMed: 15302920]
37. Rueda D, Wick K, McDowell SE, Walter NG. Diffusely bound Mg²⁺ ions slightly reorient stems I and II of the hammerhead ribozyme to increase the probability of formation of the catalytic core. *Biochemistry* 2003;42:9924–9936. [PubMed: 12924941]
38. Uhlenbeck OC. Keeping RNA happy. *Rna* 1995;1(1):4–6. [PubMed: 7489487]
39. Canny MD, Jucker FM, Pardi A. Efficient ligation of the Schistosoma hammerhead ribozyme. *Biochemistry* 2007;46:3826–3834. [PubMed: 17319693]
40. Clouet-D’Orval B, Uhlenbeck OC. Kinetic characterization of two I/II format hammerhead ribozymes. *Rna* 1996;2(5):483–491. [PubMed: 8665415]
41. Fedor MJ, Uhlenbeck OC. Kinetics of intermolecular cleavage by hammerhead ribozymes. *Biochemistry* 1992;31(48):12042–12054. [PubMed: 1280996]
42. Emilsson GM, Nakamura S, Roth A, Breaker RR. Ribozyme speed limits. *Rna* 2003;9:907–918. [PubMed: 12869701]
43. Ruffner DE, Stormo GD, Uhlenbeck OC. Sequence requirements of the hammerhead RNA self-cleavage reaction. *Biochemistry* 1990;29(47):10695–10702. [PubMed: 1703005]
44. Warashina M, Kuwabara T, Nakamatsu Y, Takagi Y, Kato Y, Taira K. Analysis of the conserved P9-G10.1 metal-binding motif in hammerhead ribozymes with an extra nucleotide inserted between A9 and G10.1 residues. *J Am Chem Soc* 2004;126:12291–12297. [PubMed: 15453762]

45. Clouet-d'Orval B, Uhlenbeck OC. Hammerhead ribozymes with a faster cleavage rate. *Biochemistry* 1997;36(30):9087–9092. [PubMed: 9254134]
46. Peracchi A, Beigelman L, Usman N, Herschlag D. Rescue of abasic hammerhead ribozymes by exogenous addition of specific bases. *Proc. Nat. Acad. Sci. USA* 1996;93:11522–11527. [PubMed: 8876168]
47. Peracchi A, Karpeisky A, Maloney L, Beigelman L, Herschlag D. A core folding model for catalysis by the hammerhead ribozyme accounts for its extraordinary sensitivity to abasic mutations. *Biochemistry* 1998;37:14765–14775. [PubMed: 9778351]
48. Gago S, De la Pena M, Flores R. A kissing-loop interaction in a hammerhead viroid RNA critical for its in vitro folding and in vivo viability. *Rna* 2005;11:1073–1083. [PubMed: 15928342]
49. Owens RA, Thompson SM, Steger G. Effects of random mutagenesis upon potato spindle tuber viroid replication and symptom expression. *Virology* 1991;185:18–31. [PubMed: 1926773]
50. Niblett CL, Dickson E, Fernow KH, Horst RK, Zaitlin M. Cross protection among four viroids. *Virology* 1978;91:198–203. [PubMed: 726264]
51. Flores R, Daros JA, Hernandez C. Avsunviroidae family: viroids containing hammerhead ribozymes. *Adv Virus Res* 2000;55:271–323. [PubMed: 11050945]
52. Gas ME, Hernandez C, Flores R, Daros JA. Processing of nuclear viroids in vivo: an interplay between RNA conformations. *PLoS Pathog* 2007;3:e182. [PubMed: 18052530]
53. Branch AD, Robertson HD. A replication cycle for viroids and other small infectious RNA's. *Science* 1984;223:450–455. [PubMed: 6197756]
54. Bussiere F, Lehoux J, Thompson DA, Skrzeczkowski LJ, Perreault J. Subcellular localization and rolling circle replication of peach latent mosaic viroid: hallmarks of group A viroids. *J Virol* 1999;73:6353–6360. [PubMed: 10400727]
55. Daros JA, Marcos JF, Hernandez C, Flores R. Replication of avocado sunblotch viroid: evidence for a symmetric pathway with two rolling circles and hammerhead ribozyme processing. *Proc Natl Acad Sci U S A* 1994;91:12813–12817. [PubMed: 7809126]

**Figure 1.**

Nine hammerheads in native context used to design nHH chimeras. Catalytic cores (red) are arranged to reflect the crystal structure (8). Stem III and immediate flanking sequences (black) are replaced in chimeras. Unique hairpins 1 and 2 (green) are also present in chimeras. rCSCVd +: (nHH1): cherry small circular RNA, PLMVd-(nHH2): peach latent mosaic viroid, satArMV + (nHH3): arabis mosaic virus small satellite RNA, satLTSV- (nHH4) and satLTSV+ (nHH8): lucerne transient streak virus satellite RNA, CChMVd+(nHH5): chrysanthemum chlorotic mottle viroid, satSCMoV+ (nHH6): subterranean clover mottle satellite RNA, satCYMoV+ (nHH7): chicory yellow mottle virus satellite RNA, satTRsV+ (nHH9): satellite of tobacco ringspot virus, where + indicates genomic strand and - indicates antigenomic strand.

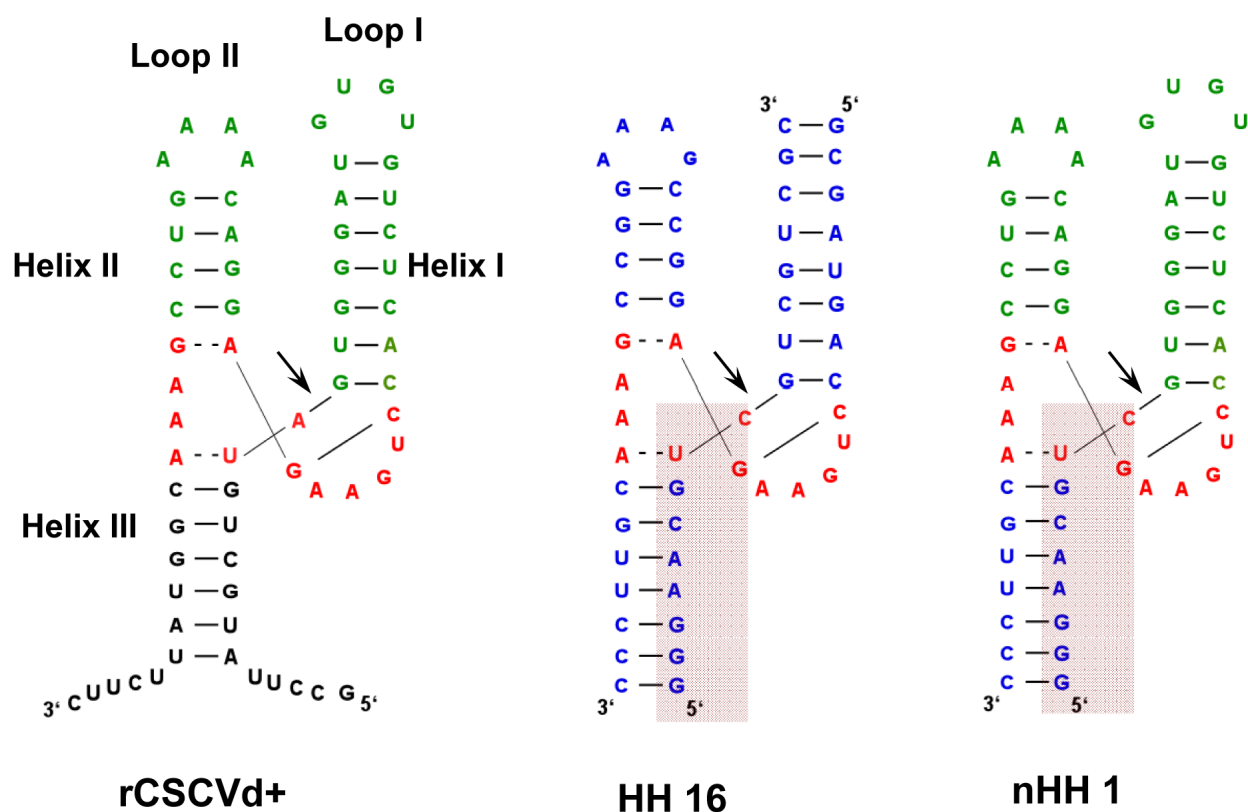
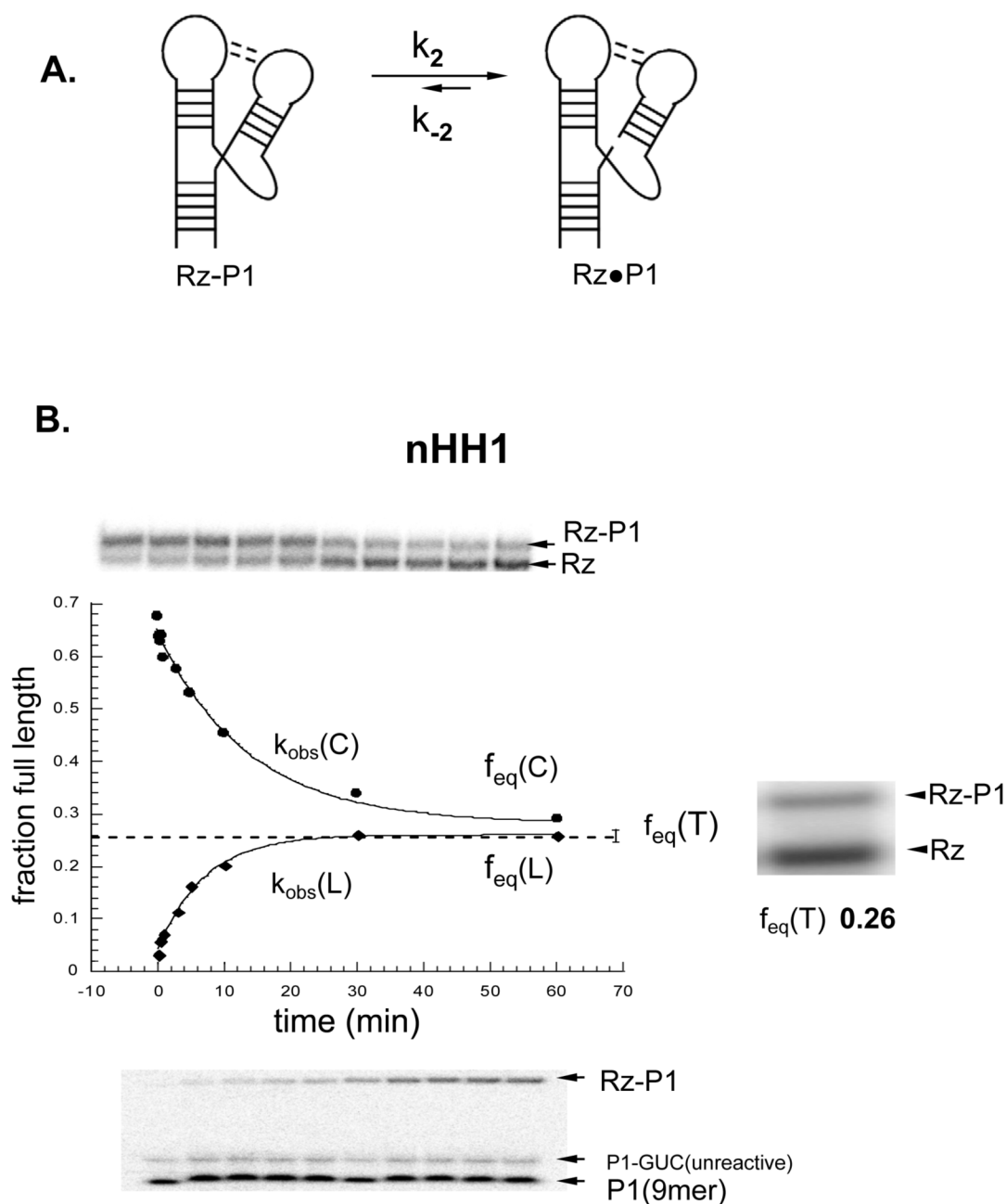


Figure 2.

Construction of nHH1 chimera from rCSCVd+ and helix III of HH16 (blue). All chimeras contain the identical nine nucleotide 5' cleavage product P1 (highlighted in the pink box on HH16 and nHH1 structures), including a C residue 3' to the cleavage site (arrow).

**Figure 3.**

Three assays of chimeric hammerheads. A. The hammerhead cleavage-ligation equilibrium. B. Example of the approach to equilibrium of nHH1 in cleavage (above) and ligation (below) in 1 mM $MgCl_2$, 50 mM MES pH 6.0. Data points are quantitation of gels and lines are single exponential fits to $k_{obs}(C) = 0.074 \text{ min}^{-1}$ and $f_{eq}(C) = 0.28$ for the cleavage reaction and $k_{obs}(L) = 0.14 \text{ min}^{-1}$ and $f_{eq}(L) = 0.26$ for the ligation reaction. Example of the coupled transcription cleavage assay (right) performed in 40 mM Tris-HCl, pH 8.1, 1 mM free $MgCl_2$ at 25° C gives $f_{eq}(T) = 0.26$.

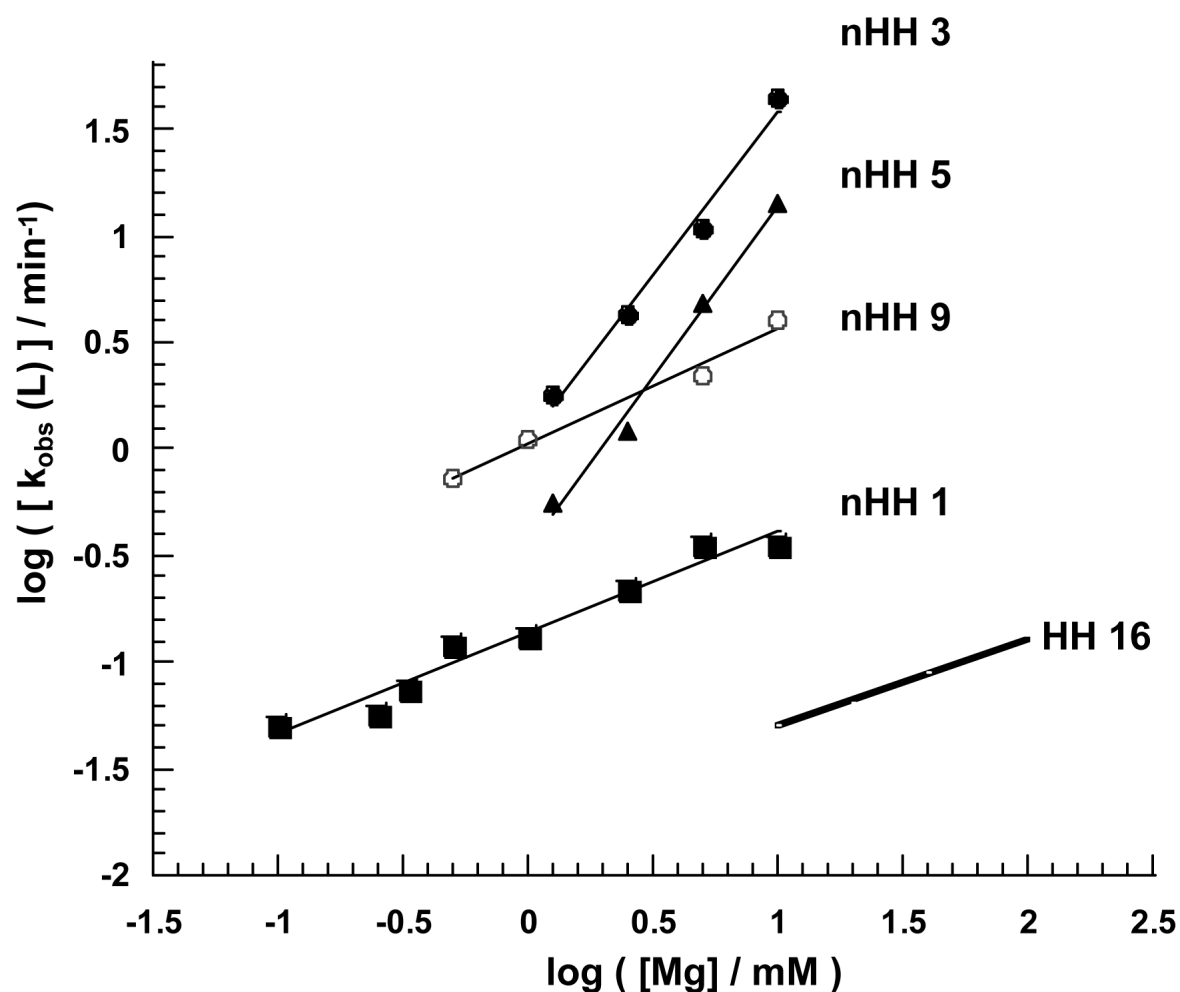


Figure 4.

A. Magnesium ion dependence of $k_{\text{obs}}(\text{L})$. Although cleavage rates for different hammerheads were determined at different pH values to maximize accuracy, the data was normalized to pH 6.0 using the log-linear pH dependence of cleavage as follows: For nHH1 and nHH9 k_{obs} was determined in 50 mM MES pH 6.0. For nHH3 and nHH5, k_{obs} values were measured at pH 5.5 and each one multiplied by 3 to correct to pH 6.0. Data for minimal HH16 previously measured at pH 7.5 (35) were corrected to pH 6.0 by dividing each rate by 30.

Table 1

Catalytic properties of chimeric hammerheads

	Ligation Assay		Cleavage Assay		Transcription Assay	
	$k_{\text{obs}}(\text{L})$ (min^{-1})	$f_{\text{eq}}(\text{L})$	$k_{\text{obs}}(\text{C})$ (min^{-1})	$f_{\text{eq}}(\text{C})$	$f_{\text{eq}}(\text{T})$	
nHH1	0.15 ± 0.05	0.32 ± 0.04	0.08 ± 0.01	0.28 ± 0.94	0.29 ± 0.04	
nHH2	1.1 ± 0.28	0.21 ± 0.06	0.89 ± 0.14	0.73 ± 0.03	0.17 ± 0.01	
nHH3	>2.5	0.01 ± 0.01	>2.5	0.79 ± 0.04	0.11 ± 0.01	
nHH4	0.66 ± 0.04	0.13 ± 0.01	0.59 ± 0.09	0.32 ± 0.03	0.17 ± 0.04	
nHH5	2.20 ± 0.18	0.005 ± 0.001	1.2 ± 0.1	0.68 ± 0.05	0.21 ± 0.02	
nHH6	1.5 ± 0.06	0.24 ± 0.006	1.2 ± 0.34	0.26 ± 0.05	0.22 ± 0.06	
nHH7	0.024 ± 0.01	0.013 ± 0.001	0.077 ± 0.03	0.79 ± 0.08	0.18 ± 0.04	
nHH8	>2.5	0.05 ± 0.002	>2.5	$0.06 \pm .004$	0.09 ± 0.01	
nHH9 ^{a)}	0.59 ± 0.10	0.06 ± 0.013	0.54 ± 0.17	0.48 ± 0.08	0.05 ± 0.002	

Cleavage and ligation assays were performed in 50 mM MES (pH 6.0) and 1 mM MgCl_2 at 25° C while transcription assays were in 40 mM Tris-HCl (pH 8.1) and 1 mM free MgCl_2 at 25° C.

^{a)} ref (19)

Table 2 $k_{\text{obs}}(\text{L})$ measured by stop flow

	pH 6.0		pH 7.3	
	1 mM MgCl_2 $k_{\text{obs}}(\text{L}) (\text{min}^{-1})$	10 mM MgCl_2 $k_{\text{obs}}(\text{L}) (\text{min}^{-1})$	1 mM MgCl_2 $k_{\text{obs}}(\text{L}) (\text{min}^{-1})$	10 mM MgCl_2 $k_{\text{obs}}(\text{L}) (\text{min}^{-1})$
nHH3	17 ± 2	30 ± 3	560 ± 60	860 ± 100
nHH8	6.8 ± 1.2	20 ± 4	200 ± 160	470 ± 110

Table 3
Calculation of cleavage and ligation rate constants and K_{int}

	$k_{obs}(\text{min}^{-1})$	f_{eq}	$k_2(\text{min}^{-1})$	$k_2(\text{min}^{-1})$	K_{int}
nHH1	0.15	0.29	0.11	0.042	2.4
nHH2	1.1	0.17	0.91	0.19	4.9
nHH3	17	0.11	15	1.9	8.1
nHH4	0.66	0.17	0.55	0.11	5.0
nHH5	2.2	0.21	1.7	0.46	3.8
nHH6	1.5	0.22	1.2	0.33	3.5
nHH7	0.024	0.18	0.02	0.004	4.6
nHH8	6.8	0.09	6.2	0.61	10
nHH9 ^a	0.59	0.03	0.57	0.018	32
HH16 ^b	0.004	0.0075 ^c	0.004	3×10^{-5}	130

All values given at 25° C in 1 mM MgCl₂, 50 mM MES, pH 6.0. Values of k_{obs} and f_{eq} are best estimates based on data in Tables 1 and 2.

^a ref (19).
^b ref (35).
^c ref (21).

Table 4 $k_{\text{obs}}(\text{L})$ in 2M LiCl

Hammerhead	$k_{\text{obs}}(\text{min}^{-1})$
nHH1	0.12 ± 0.01
nHH2	0.22 ± 0.04
nHH3	0.32 ± 0.1
nHH4	0.12 ± 0.04
nHH5	0.16 ± 0.05
nHH6	0.38 ± 0.08
nHH7	0.0086 ± 0.002
nHH8	0.35 ± 0.02
nHH9	0.16 ± 0.06
HH8 ^{a)}	0.05

Rates determined in 50 mM HEPES, pH 7.5, 2 M LiCl at 25° C.

^{a)}_{ref (18)}